2014
23rd International Lightning Detection Conference
18 - 19 March • Tucson, Arizona, USA
5th International Lightning Meteorology Conference
20 - 21 March • Tucson, Arizona, USA

Lightning NO_x Production Per Flash based on OMI NO_2 Observations and Ground Network Lightning Data

Kenneth Pickering
Atmospheric Chemistry and Dynamics Laboratory
NASA Goddard Space Flight Center
Greenbelt, Maryland USA
Kenneth.E.Pickering@nasa.gov

Dale Allen, Allison Ring
Department of Atmospheric and Oceanic Science
University of Maryland
College Park, Maryland USA

Eric Bucsela
SRI, International
Menlo Park, California USA

Amitabh Nag, Ron Holle
Vaisala, Inc.

Abstract— **Lightning production of nitrogen oxides (NO_x) in the middle and upper troposphere contributes significantly to the production of ozone which is an important greenhouse gas in this region of the atmosphere. Improved estimates of the lightning NO_x (LNO_x) produced per flash are imperative to determine the natural source strength of NO_x and ultimately upper troposphere ozone. An algorithm to derive LNO_x from data observed by the Ozone Monitoring Instrument (OMI) onboard NASA's Aura satellite has been developed. Key elements of the algorithm include subtraction of the stratospheric and tropospheric background components from the total column NO_2, and the use of an air mass factor appropriate for LNO_x to convert the satellite-measured slant column amount to a vertical column amount.**

Daily data sets containing OMI LNO_x estimates on a 2 x 2.5 degree grid were generated for an initial study area, the Gulf of Mexico, and compared to lightning flash rates derived from ground network (e.g., GLD360) lightning data adjusted for detection efficiency relative to the Optical Transient Detector and Lightning Imaging Sensor (OTD/LIS). Estimates of LNO_x production per flash are generated using gridded total flashes for 6 hour periods prior to OMI overpass in conjunction with the OMI-based LNO_x fields. These estimates of LNO_x production in moles per flash are compared with literature values.

Keywords—nitrogen oxides, ozone, GLD360, OMI

I. INTRODUCTION

NO_2 and NO (together referred to as NO_x) are trace gases important in ozone chemistry in both the troposphere and stratosphere. Worldwide, anthropogenic emissions of NO_x dominate the NO_x budget. However, considerable uncertainty surrounds emission rates from natural sources (lightning and soil). Lightning is the largest non-anthropogenic source of NO_x in the free troposphere (hereafter, we refer to lightning-generated NO_x as LNO_x). Most estimates of global LNO_x production range from 2 to 8 Tg (N) yr^{-1} (Schumann and Huntrieser, 2007) or about 10–15% of the total NO_x budget. The effects of lightning are felt most strongly in the middle and upper part of the troposphere, where this source plays the dominant role in controlling NO_x and ozone amounts especially in the tropics and at midlatitudes in the summer, despite the greater overall magnitude of the anthropogenic NO_x emissions (R. Zhang et al., 2003). In this region, NO_x has a lifetime several times longer than the approximate 1-day lifetime in the lower troposphere so that a given amount of LNO_x in the upper troposphere can have a greater impact on ozone chemistry. Ozone is the third most important greenhouse gas (IPCC, 2007), and ozone enhancements near the tropopause have the greatest effect on its radiative forcing. Therefore, additional ozone produced downwind of thunderstorm events is particularly effective in climate forcing.

Two types of information are needed for estimating the global LNO_x source strength: the global flash rate and the production per flash. The global number of flashes is fairly well established as a result of climatologies constructed from satellite sensors such as the Optical Transient Detector (OTD, 1995-2000) (Christian et al., 2003; Boccippio et al., 2000) and the Lightning Imaging Sensor (LIS, 1997 to present) (Christian et al., 2003; Boccippio et al., 2002; Mach et al., 2007). Therefore, the factor of 4 uncertainty in the range of global LNO_x source strength stems primarily from uncertainty in the NO_x production per flash. There have been several methods used to estimate this quantity: theoretical estimates, laboratory experiments, analysis of aircraft observations, cloud-resolving model simulations constrained by lightning flash observations and anvil NO_x measurements, and analysis of satellite observations (see Table 1). Our group has employed the latter three of these methods in previous analyses of LNO_x production. Under NASA-sponsored work, we have developed a preliminary algorithm for computing LNO_x from OMI observations and have applied it for sets of tropical (Bucsela et al., 2010) and midlatitude convective storms. From Table 1 it can be noted that in general, estimates of average LNOx production per flash determined for midlatitude and subtropical thunderstorms tend to be larger than for tropical thunderstorms. Huntrieser et al. (2008) have hypothesized that LNOx production per flash at midlatitudes may be larger than in the tropics due to greater vertical wind shear at higher latitudes, leading to greater flash lengths.

II. ALGORITHM

The Ozone Monitoring Instrument (OMI) is on NASA's Aura satellite, which is part of NASA's A-Train. It is in a sun-synchronous polar orbit, crossing equator at 1:30pm (LT). NO_2 and other species are retrieved using UV/VIS radiance observations. OMI provided daily global coverage beginning in late 2004. However, a substantial number of the pixels in the field of view became blocked after 2008, reducing the coverage per day. The OMI pixel at nadir is 13 x 24 km; pixels become larger toward the edges of the orbital swath. The NASA standard product retrieval for NO_2 (Bucsela et al., 2013) provides the total slant column amount of NO2 between the satellite and the earth's surface, as well as stratospheric and tropospheric vertical column amounts.

We have developed a special algorithm to retrieve the component of NO_2 due to lightning and convert this to a vertical column of NO_x.

$$\Omega_{LNOx} = \frac{\Omega_{total}^{slant} - \Omega_{strat}^{OMI} \times AMF_{strat} - \Omega_{BG}^{OMI} \times AMF_{trop}}{AMF_{LNOx}}$$

In this equation Ω is the column amount (which can be either NO_X or NO_2). The stratospheric column (red) is based on mean OMI stratospheric NO_2 from the standard algorithm for 4 days surrounding day of analysis. The tropospheric background (BG) column (green) is an estimate of the contributions of sources other than lightning to tropospheric column. We use the monthly mean tropospheric NO_2 column from the standard algorithm as an approximation of the background. For both stratosphere and tropospheric background we use the air mass factors (AMF) supplied by the standard algorithm to convert the vertical columns to slant columns. AMFs result from radiative transfer modeling using an assumed NO_2 profile, cloud information, and surface albedo. We consider all OMI pixels regardless of cloud amount. Following subtraction of the stratospheric and tropospheric background components in the numerator, we divide by an AMF for LNO_X, which assumes a profile shape appropriate for LNO_x (maximum in the upper troposphere). This AMF converts the slant column LNO_2 to vertical column LNO_x. The LNO_x profile shape comes from gridded output from NASA's Global Modeling Initiative (GMI) chemical transport model which was run with and without lightning. Profiles of LNO and LNO_x are obtained by subtracting the profiles from the no-lightning simulation from those from the simulation with lightning. Our algorithm results in vertical LNO_X columns for each OMI pixel.

For the purposes of our study, we sum the LNO_x production over the 2 x 2.5 degree grid cells of the GMI model. We also make the assumption that lightning flashes occurring over the six hours prior to OMI overpass in a given grid cell contribute to the LNOx derived for that cell. These flash counts are derived from GLD360 observations (Demetriades et al., 2010; Said et al., 2013). Allen et al. (2014) describe how the detection efficiency of the GLD360 stroke data is determined relative to the OTD/LIS climatology. Detection efficiencies to convert observed GLD360 strokes to flashes were determined for each GMI grid cell as a function of time. For each grid cell on each day, we compute LNO_x production per flash by dividing the LNOx from our algorithm by the number of GLD360 six-hour adjusted flashes in each grid cell.

III. RESULTS

We have obtained GLD360 data for a region over the Gulf of Mexico and its surroundings for the period from May 2011 through September 2013. We have analyzed the LNO_x per flash in this region each day during July 2011, and have produced very preliminary results. Figure 1 shows maps of the 6-hour flashes (adjusted for detection efficiency) and the OMI LNO_x for July 3, 2011. Large adjusted flash rates are seen over the Gulf of Mexico offshore from Louisiana, peaking at over 13,000 flashes in one grid cell in the six hours prior to OMI overpass. Substantial OMI LNO_x per grid cell also is evident over a large area of the Gulf. A maximum of over 1000 kmoles LNO_x per grid cell stretches southward from the Louisiana coastal area. Over the domain shown in Figure 1 the average LNO_x production per flash on this day was 322.4 moles per flash. This value is within the range of LNO_x production per flash seen in prior studies, such as those listed in Table 1.

Figure 2 shows similar maps for July 15, 2011 over the Gulf of Mexico. On this day two primary areas of adjusted GLD360 flashes are seen. One region stretches from Houston, TX eastward across Louisiana, and the second is off the east coast of Florida. LNO_x is retrieved from OMI in both of these

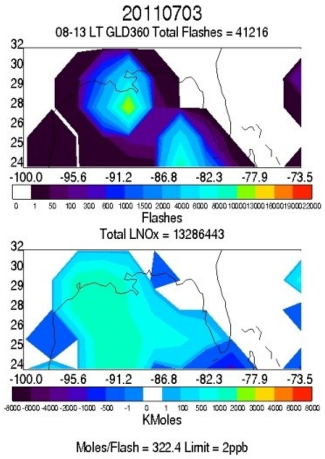

Figure 1. GLD360 adjusted flashes for the six hours prior to OMI overpass (top) and OMI LNO_x (bottom) for Gulf of Mexico region on July 3, 2011

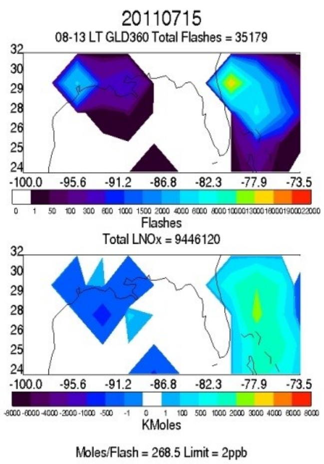

Figure 2. GLD360 adjusted flashes for the six hours prior to OMI overpass (top) and OMI LNOx (bottom) for Gulf of Mexico region on July 15, 2011.

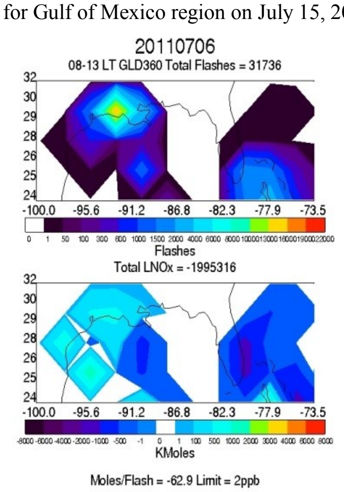

Figure 3. GLD360 adjusted flashes for the six hours prior to OMI overpass (top) and OMI LNOx (bottom) for Gulf of Mexico region on July 6, 2011.

regions. The maximum LNO_x over the Atlantic east of Florida is over 3000 kmoles per grid cell and is located to the southeast of the flash maximum. Over the Gulf domain the mean LNO_x production per flash on this day is 268.5 moles/flash, which is also comparable to many of the literature values.

However, on some days during July 2011, the mean LNO_x production per flash is negative. Figure 3 shows an example of this type of occurrence on July 6, 2011. Strong flash and OMI LNO_x maxima are indicated over southwestern Louisiana. However, the flash maximum over southern Florida is accompanied by negative values of LNO_x. We are currently investigating the reason for this result from our algorithm. Two terms are subtracted from the total slant column NO2 in the numerator. We do not believe that at the latitude range of the Gulf of Mexico in midsummer the stratospheric term is to blame for the negative results, as the stratosphere has weak gradients in this region at this time of year. More likely, it is the tropospheric background that has been poorly estimated over the highly populated area of south Florida. The monthly mean OMI tropospheric NO_2 column may not have been representative of background on this day. Further investigation is in progress.

IV. SUMMARY

Very preliminary results of our analysis of OMI-based LNO_x/flash in association with GLD360 adjusted flash rates for the Gulf of Mexico region have been obtained for the month of July 2011. During this month the LNO_x/flash on a number of the days examined fell within the range of previous studies. However, we also obtain significantly negative values on some days. We are currently investigating the reasons why we see large negative values. The initial hypothesis is that we need a better method of estimate for the tropospheric background. We are also currently focusing on case studies of storms observed with aircraft NO_x measurements during the 2012 Deep Convective Clouds and Chemistry (DC3). Comparisons of LNO_x observed by aircraft with those from OMI should inform us of how to improve our algorithm.

ACKNOWLEDGMENT

This research is supported by the NASA Aura Science Team project.

REFERENCES

Allen, D., A. Ring, K. Pickering, A. Nag, R. Holle, R. Holzworth (2014) Analysis of Ground Network Lightning Data Relative to OTD/LIS to Derive Flash Rates for Use in Determining Lightning NO_x Production from Satellite Observations, ILDC/ILMC, Tucson, AZ.

Beirle, S., N., et al. (2006), Estimating the NOx produced by lightning from GOME and NLDN data: A case study in the Gulf of Mexico, *Atmos. Chem. Phys.*, *6*, 1075–1089.

Beirle, S., H. Huntrieser, and T Wagner (2010), Direct satellite observation of lightning-produced NOx, *Atmos. Chem. Phys*., 10(22), 10965-10986, doi:10.5194/acp-10-10965.

Boccippio, D., K. Driscoll, W. Koshak, R. Blakeslee, W. Boeck, D. Mach, D. Buechler, H. J. Christian, and S. J. Goodman (2000), The Optical

Transient Detector (OTD): Instrument Characteristics and Cross-Sensor Validation, *J. Atmos. Oceanic Tech.*, *17*, 441-458.

Boccippio, D. J., W. J. Koshak, and R. J. Blakeslee (2002), Performance assessment of the Optical Transient Detector and Lightning Imaging Sensor, I: Predicted diurnal variability, *J. Atmos. Oceanic Technol.*, *19*, 1318–1332

Bucsela, E. J., K. E. Pickering, et al. (2010), Lightning-generated NOx seen by OMI during NASA's TC4 experiment, *J. Geophys. Res*., doi:10.1029/2009JD013118, in press.

Bucsela, E. J., N. A. Krotkov, E. A. Celarier, L. N. Lamsal, W. H. Swartz, P. K. Bhartia, K. F. Boersma, J. P. Veefkind, J. F. Gleason, and K. E. Pickering, (2013) A new stratospheric and tropospheric NO2 retrieval algorithm for nadir-viewing satellite instruments: applications to OMI, *Atmos. Meas. Tech. Discuss*., 6, 1361–1407, www.atmos-meas-tech-discuss.net/6/1361/2013/doi:10.5194/amtd-6-1361-2013.

Christian, H. J., et al. (2003), Global frequency and distribution of lightning as observed from space by the Optical Transient Detector, *J. Geophys. Res.*, *108* (D1), 4005, doi:10.1029/2002JD002347.

DeCaria, A. J., K. E. Pickering, G. L. Stenchikov, and L. E. Ott (2005), Lightning-generated NOx and its impact on tropospheric ozone production: A three-dimensional modeling study of a STERAO-A thunderstorm, *J. Geophys. Res*., *110*, D14303, doi:10.1029/2004JD005556.

Demetriades, N. W. S., M. J. Murphy, and J. A. Cramer (2010) Validation of Vaisala's global lightning dataset (GLD360) over the continental United States. Proc. 21st Int. Lightning Detection Conf., Orlando, FL, Vaisala, 6 pp.

Huntrieser, H., U. Schumann, H. Schlager, H. Höller, A. Giez, H.-D. Betz, D. Brunner, C. Forster, O. Pinto Jr., and R. Calheiros (2008), Lightning activity in Brazilian thunderstorms during TROCCINOX: Implications for NOx production, *Atmos. Chem. Phys.*, *8*, 21–953.

Huntrieser, H., et al. (2009), NOx production by lightning in Hector: first airborne measurements during SCOUT-O3/ACTIVE, *Atmos. Chem. Phy*s., 9, 8377-8412

Huntrieser, H., H. Schlager, M. Lichtenstern, M., P. Stock, T. Hamburger, H. Höller, K. Schmidt, H.-D. Betz, A. Ulanovsky, and F. Ravegnani (2011), Mesoscale convective systems observed during AMMA and their impact on the NOx and O-3 budget over West Africa, *Atmos. Chem. Phys*., 11, 2503-2536, doi:10.5194/acp-11-2503.

IPCC (2007), *Contribution of Working Group I to the Fourth Assessment Report of the Intergovernmental Panel on Climate Change*, 2007, S. Solomon, D. Qin, M. Manning, Z. Chen, M. Marquis, K.B. Averyt, M. Tignor and H.L. Miller (eds.), Cambridge University Press, Cambridge, United Kingdom and New York, NY, USA.

Koshak, W., H. Peterson, A. Biazar, M. Khan, and L. Wang (2013), The NASA Lightning Nitrogen Oxides Model (LNOM): Application to air quality modeling, *Atmos. Res.,* http://dx.doi.org/10.1016/j.atmosres.2012.12.015.

Mach, D. M., H. J. Christian, R. J. Blakeslee, D. J. Boccippio, S. J. Goodman, and W. L. Boeck (2007), Performance assessment of the Optical Transient Detector and Lightning Imaging Sensor, *J. Geophys. Res.*, *112*, D09210, doi:10.1029/2006JD007787.

Ott, L. E., K. E. Pickering, G. L. Stenchikov, H. Huntrieser, and U. Schumann (2007), Effects of lightning NOx production during the 21 July European Lightning Nitrogen Oxides Project storm studied with a three-dimensional cloud-scale chemical transport model, *J. Geophys. Res.*, *112*, D05307, doi:10.1029/2006JD007365.

Ott, L. E., K. E. Pickering, G. L. Stenchikov, D. J. Allen, A. J. DeCaria, B. Ridley, R.-F. Lin, S. Lang, and W.-K. Tao (2010), Production of lightning NOx and its vertical distribution calculated from three-dimensional cloud-scale chemical transport model simulations, *J. Geophys. Res*., *115*, D04301,doi:10.1029/2009JD011880.

Price, C., J. Penner, and M. Prather (1997), NOx from lightning 1. Global distribution based on lightning physics, *J. Geophys. Res*., *102* (D5), 5929-5941.

Said, R. K., M. B. Cohen, and U. S. Inan (2013), Highly intense lightning over the oceans: Estimated peak currents from global GLD360 observations, *J. Geophys. Res. Atmos.*, *118*, doi:10.1002/jgrd.50508.

Schumann, U., and H. Huntrieser (2007), The global lightning-induced nitrogen oxides source, *Atmos. Chem. Phys*., *7*, 3823-3907.

Wang, Y., A. W. DeSilva, G. C. Goldenbaum, and R. R. Dickerson (1998), Nitric oxide production by simulated lightning: Dependence on current, energy and pressure, J. *Geophys. Res.*, 103, 19,149– 19,159.

Zhang, R., X. Tie, and D. W. Bond (2003), Impacts of anthropogenic and natural NOx sources over the U.S. on tropospheric chemistry, *Proc. Natl. Acad. Sci. U.S.A.*, *100* (4), 1505-1509, doi:10.1073/pnas.252763799. Abarca, S. F. K. L. Corbosiero, and T. J. Galameau Jr. (2010), An evaluation of the WWLLN using the NLDN as ground truth, *J. Geophys. Res*., 115, D18206, doi:10.1029/2009JD013411.

Table 1. Some Literature Estimates of LNO_x Production Per Flash

Method	Moles NO/flash (Notes)	Reference
Theoretical	1100 (CG), 110 (IC)	Price et al., 1997
Laboratory	~103	Wang et al., 1998
Aircraft data, cloud model	345-460 (STERAO-A)	DeCaria, et al., 2005
Aircraft data, cloud model	360 (STERAO-A, EULINOX)	Ott et al., 2007; 2010
Aircraft data, cloud model	590-700 (CRYSTAL-FACE)	Ott et al., 2010
	500 (Mean midlat. from model)	Ott et al., 2010
Aircraft data, cloud model	500 - 600 (Hector)	Cummings et al., 2013
Aircraft data	70-210 (TROCCINOX)	Huntrieser et al., 2008
Aircraft data	121-385 (SCOUT-O3 Darwin)	Huntrieser et al., 2009
Aircraft data	70-179 (AMMA)	Huntrieser et al., 2011
LMA/Theoretical	484 (CG), 34 (IC)	Koshak et al., 2013
Satellite (GOME)	32-240 (Sub-Tropical)	Beirle et al., 2006
Satellite (OMI)	87-246 (TC4 – tropical marine)	Bucsela et al., 2010
	174 (TC4 mean from OMI)	Bucsela et al., 2010
Satellite (OMI)	440 (Central US, Gulf)	Pickering et al. (in prep)
Satellite (SCIAMACHY)	33-50 max. (global analysis)	Beirle et al., 2010